

# Predictive Analytics on Real-Time Biofeedback for Actionable Classification of Activity State

William M. Mongan

Advisor: Adam K. Fontecchio

Examining Committee: Kapil R. Dandekar (chair), Genevieve Dion,  
Nagarajan Kandasamy, Timothy Kurzweg



DREXEL UNIVERSITY  
College of  
Engineering

3/10/2019

| 1

# Outline

- **Introduction and Background**
- Secure and Efficient Monitoring of RFID-Based Devices
- Feature Extraction from Physical Properties of RFID
- State Classification
- Rate Estimation
- Prediction
- Experimental Protocol
- Conclusions and Contributions



# Wearable Smart Garments for Health Monitoring on the Internet of Things (IoT)

- The problem: currently, medical monitoring devices such as uterine monitors or respiratory monitors are tethered to a monitoring unit:
  - ... requiring that the wearer remain somewhat stationary, increasing the risk of blood clotting
  - ... restricting ambulatory periods such as restroom breaks, unless monitoring is discontinued
- Wireless monitoring devices have emerged, but require a battery or rechargeable battery source.
  - Wearable technology often consists of a watch, or sensor, attached to the clothing.
  - Monitoring devices look for readings “outside the normal range” and alert the parents, perhaps unnecessarily.



<https://5.s.portea.com/medical-equipment/wp-content/uploads/2016/07/DVT-Deep-Vein-Thrombosis-Pump-4-400x400.jpg>



[https://cdn.shopify.com/s/files/1/0284/7802/products/Fichier\\_69\\_1024x1024.png?v=1523107307](https://cdn.shopify.com/s/files/1/0284/7802/products/Fichier_69_1024x1024.png?v=1523107307)



[https://cdn.shopify.com/s/files/1/1004/3036/files/Owlet\\_group\\_800x.png?v=1523396589](https://cdn.shopify.com/s/files/1/1004/3036/files/Owlet_group_800x.png?v=1523396589)

[http://www.wearables.com/wp-content/uploads/2015/06/8c874d764787dc39\\_ces2014-restdevices\\_mimo-0621.jpg.xxlarge\\_2x.jpg](http://www.wearables.com/wp-content/uploads/2015/06/8c874d764787dc39_ces2014-restdevices_mimo-0621.jpg.xxlarge_2x.jpg)



[https://i0.wp.com/houndhill.com/wp-content/uploads/2013/07/shapeimage\\_3.png?resize=274%2C212](https://i0.wp.com/houndhill.com/wp-content/uploads/2013/07/shapeimage_3.png?resize=274%2C212)



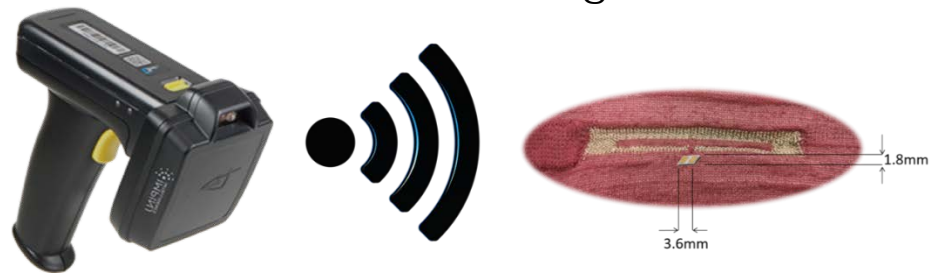
# Wearable Smart Garments for Health Monitoring on the Internet of Things (IoT)

- “Normal range” varies by the wearer, but monitoring is often done on-demand.
  - Devices are often used when needed, which is not conducive for baselining.
  - The 95% body temperature range was 96.3-99.1° F (mean 97.8° F), with age, race, and gender correlations in a study of 35,000 patients (Z. Obermeyer, *et al*, BMJ 2017;359:j5468).
    - 8.2% of variation were explained by comorbidities.
- Normal respiratory, temperature, and pulse ranges are wide and vary with age and physical activity.
  - A 1° C increase in body temperature correlates to an additional 10 beats per minute in a study of 31,000 children (P. Davies and I. Maconochie, EMJ 2009; 26).
- Relationships between heart rate, skin temperature, and blood glucose concentration suggest that wearable monitors can aid in management of Type 1 Diabetes during aerobic exercise (K. Turksoy, *et al*, Sensors 2017; 17(3):352).



# Wearable Smart Garments for Health Monitoring on the Internet of Things (IoT)

- Passive wireless technologies such as some Radio Frequency Identification (RFID) tags harvest power from the wireless signal, enabling inventory tracking without an external power source.
- Passive RFID repeatedly:
  - powers a small state machine on a chip from the interrogation signal,
  - does rudimentary coordination with other RFID chips in the field to avoid collisions, and
  - encodes an identification code into the reflected signal back to the interrogator.
- Poll repeatedly to prevent signal loss due to collisions.



<http://www.impinj.com/media/3533/tsl-1128-smallest-main-product-image.png>



## Challenges with Sensing via RFID

- RFID physical tag response properties change as the tag moves in space.
  - Phase, Doppler shift, Received Signal Strength Indicator (RSSI)
- A tag placed near the body exhibits oscillatory or other artifacts as the body moves.
  - Unfortunately, the tag properties also change even in a static environment, due to multipath fading and shadowing.
- A knitted metallic thread antenna is placed into a wearable “smart garment device,” deployed about the RFID tag.
  - This antenna is shaped for optimal impedance matching to the RFID tag at a single frequency in the UHF RFID band (902-928 MHz).
  - We are required to “channel hop” every 200 ms over 50 500 kHz channels in this band.
  - The backscattered signal can be weak due to the proximity to the body and the small movements to the knit antenna involved in human respiration, rather than to the tag itself.



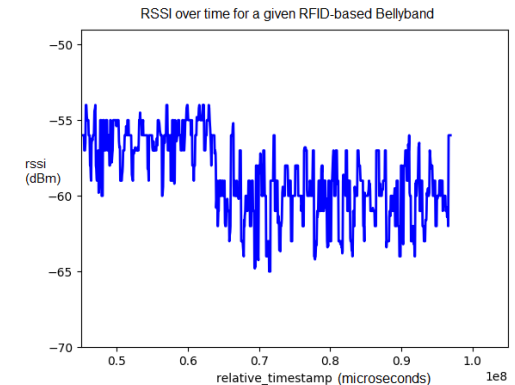
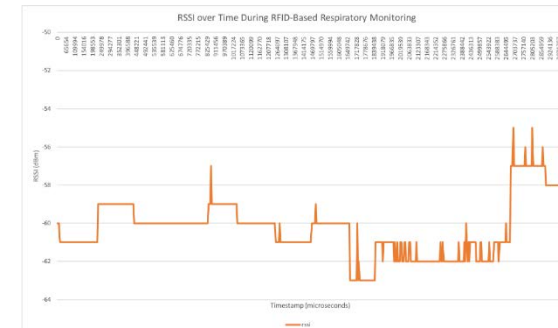
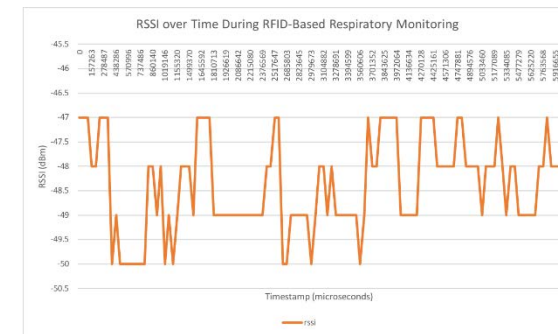
<https://images-na.ssl-images-amazon.com/images/I/11Rq1%2BmKOeL.jpg>

[https://cdn2.bigcommerce.com/n-ww20x/ka7ofex/products/1316/images/5005/Impinj\\_Speedway\\_Revolution\\_R420\\_Reader\\_2\\_port\\_\\_73229.1453405918.480.480.png?c=2](https://cdn2.bigcommerce.com/n-ww20x/ka7ofex/products/1316/images/5005/Impinj_Speedway_Revolution_R420_Reader_2_port__73229.1453405918.480.480.png?c=2)



# Challenges with Sensing via RFID

- As the wearer breathes, the shape of the knitted antenna deforms, degrading the impedance match and the physical properties of the weakened RF backscatter response.
  - ... as does a change in frequency.
- Additionally, observed changes in RF backscatter properties are subject to variation in wearer fit and positioning.
- RF backscatter properties change as the tag itself moves in space.
  - Unrelated movements by the wearer also result in perturbations in the backscatter signal properties being monitored.
- Our goal is to monitor the return loss, distance, and antenna shape via the physical properties reported by the RFID interrogator.
  - Off-the-shelf interrogators report limited, quantized measurements.
  - Changes in antenna shape, position, and interrogator occur simultaneously.



## State of the Art

- Existing work in RFID-based localization uses Angle of Arrival (AoA) information available on other interrogators or by using multiple interrogation antennas, fused with eigenspace methods like MUSIC or maximum likelihood methods.
- Many wearable sensors are portable devices tethered to the human body, such as an acoustic tracheal sensor to detect snoring spells with 89% accuracy.
  - Others are “contactless,” but assume a fixed deployment for controlled study.
- Many RFID-based localization sensors assume a fixed frequency in the 900 MHz band and a multi-sensor deployment, bypassing deployment challenges with SDR.
  - Other RFID-based monitors detect coarse movements or behaviors.
- non-RFID wireless protocols are sometimes used with success, for example, the WiBreathe system, but this assumes that subjects are a certain distance apart, and use multiple active transceivers.
- A knitted fabric antenna enables mobility and ubiquity, but degrades the signal due to absorption, and requires sensing fine movements of the antenna rather than coarse movements of the tag itself.



E. Rodriguez, *et al*, BMJ 2014;4:e005299

## State of the Art

- For example, Uysal and Filik (ELECO 2017) use a constant 900 MHz band signal from two active Software Defined Radios (SDR) acting as transmitter/receiver to monitor respiratory patterns on a human body.
  - Active transmitters off of the human body enable a high signal to noise ratio in which outlier spikes are removed via Hampel Identifier.
  - Noise is separated from the signal via eigen decomposition by the MUSIC algorithm.
  - Respiratory rate is estimated via maximum likelihood (MLE) of FFT.
  - Although the deployment is contactless on the human body, the body must be within range of the two radios and mobility is assumed to be captured as a noise vector by the MUSIC algorithm.
  - An unobtrusive wearable device causes noise in the system that is not well separated by MUSIC, but enables subject mobility.
  - Frequency hopping in the 900 MHz band introduces noise artifacts.
  - FFT MLE estimation is a subject of our prior work (SPMB 2016).
- These approaches require either more sophisticated RFID interrogation equipment, additional infrastructure per deployment, or training data in order to perform classification.



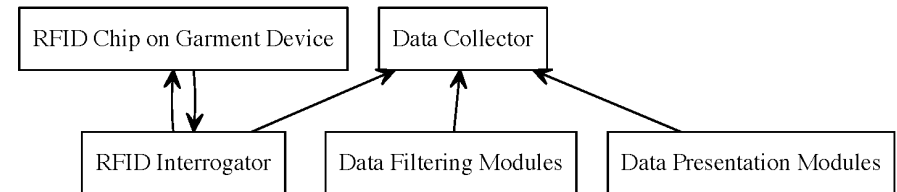
## Outline

- Introduction and Background
- **Secure and Efficient Monitoring of RFID-Based Devices**
- Feature Extraction from Physical Properties of RFID
- State Classification
- Rate Estimation
- Prediction
- Experimental Protocol
- Conclusions and Contributions

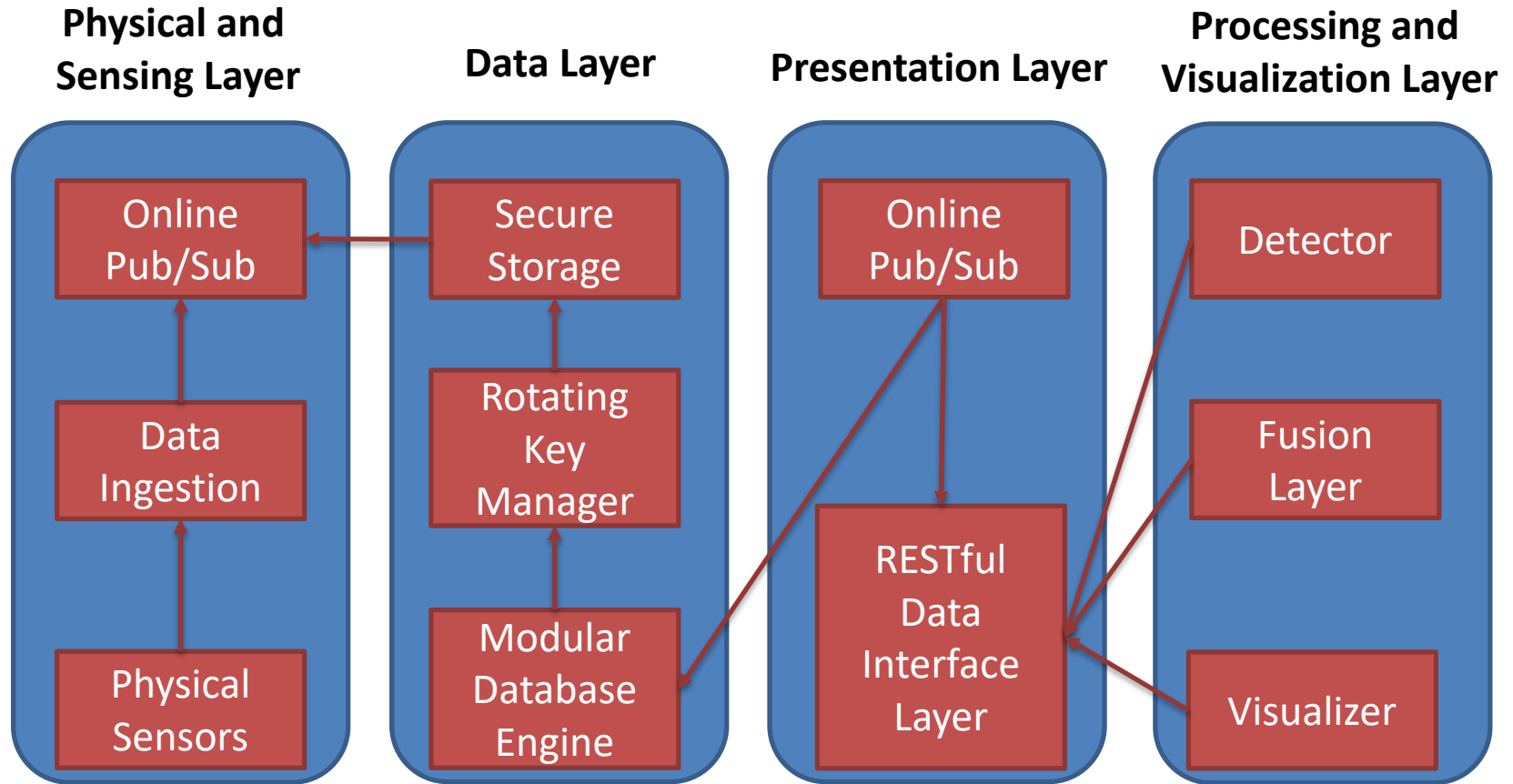


## Secure and Efficient Monitoring of RFID-Based Devices

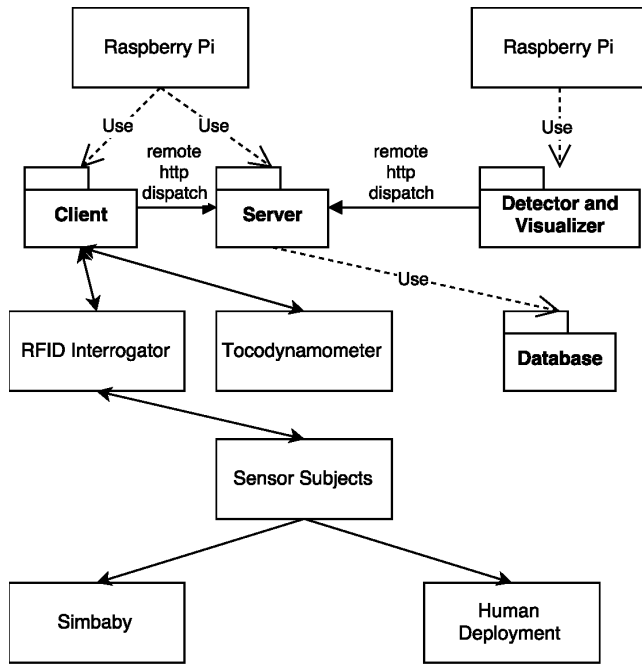
- Data collected and stored for biomedical processing must be stored in a framework that is:
  - HIPAA compliant, and
  - capable of polling RFID tags as quickly as possible to maximize the sampling rate used to observe small changes in backscatter properties.
- We must be able to drive and sample from a heterogeneous suite of sensors in real-time.
  - As the sampling rate increases, the network overhead from the interrogator devices, as many interrogators transmit tags one-by-one as they are received.
  - Configuring the interrogator to send tags in batch often results in aggregation of the RF backscatter properties, because they are assumed by the interrogator to be irrelevant to the application layer.
- We restrict ourselves to a single RFID interrogator, antenna, and knitted chip antenna.



# Secure and Efficient Monitoring of RFID-Based Devices

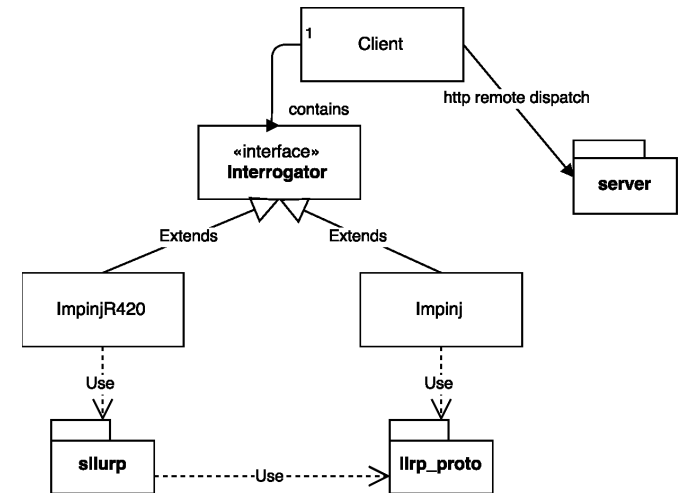


# Physical and Sensing Layer



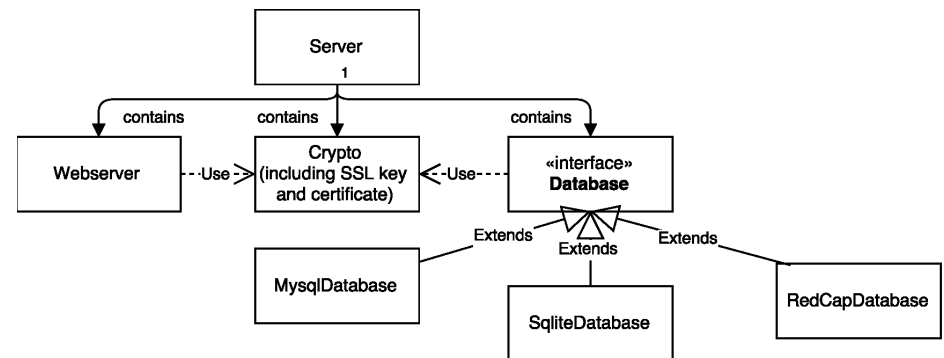
- The Low Level Reader Protocol (LLRP) library (*slurp*) was modified to implement a message queue, combining the Producer-Consumer pattern with a Top-Half/Bottom-Half processing paradigm.

- Client drivers for the Impinj interrogator was modified to augment measurement reports with Doppler and Phase fields.



## Data and Presentation Layers

- RF backscatter properties are treated as potentially Protected Health Information (PHI) under HIPAA law, and is password protected/logged.
  - A symmetric key alone would not be useful, since the ciphertext would reveal the same patterns as the unencrypted numerical data, so a block cipher is used.
  - To enable decrypting individual blocks of data during random access, a rotating temporary one-time password (TOTP) is generated dynamically and used as a salt in conjunction with the user password.
- The database is exposed via live RESTful web services using HTTP over SSL.
- By disabling Nagle's algorithm for transport, we control data throughout and prevent buffering of small messages (such as a single interrogation report) for arbitrary periods of time.



# Outline

- Introduction and Background
- Secure and Efficient Monitoring of RFID-Based Devices
- **Feature Extraction from Physical Properties of RFID**
- State Classification
- Rate Estimation
- Prediction
- Experimental Protocol
- Conclusions and Contributions

Processing and  
Visualization Layer



# Feature Extraction from Physical Properties of RFID: Signal Model

- To overcome confusion in the signal, the signal model incorporates the transmission frequency according to the Friis Transmission Formula:

$$P_{rx} = P_{tx} G_{rx}^2 G_{tag}^2 \left( \frac{\lambda}{4\pi r} \right)^4 R$$
$$G = (4\pi A) / \lambda^2$$

$$v = \frac{\lambda f_m}{2 \cos(\alpha)}$$

- Channel-corrected received power  $\zeta$  is obtained by combining Friis Transmission Formula with the equation relating gain and aperture, and separating constant terms from those that change with antenna movement:

$$\zeta = \frac{r^4}{A_{tag}^2 R} = \frac{P_{tx} A_{rx}^2}{P_{rx} \lambda^4}$$

- P: power (Watts)
- G: gain (dB)
- c: speed of light in a vacuum
- $\lambda$ : interrogation wavelength (meters) (c/frequency "f" in Hz)
- r: interrogation radius (meters)
- R: return loss (dB)
- v: tag "velocity" (meters/second)
- A: effective aperture (meters<sup>2</sup>)
- $\alpha$ : interrogation angle (radians)
- $f_m$  Doppler shift (Hz)



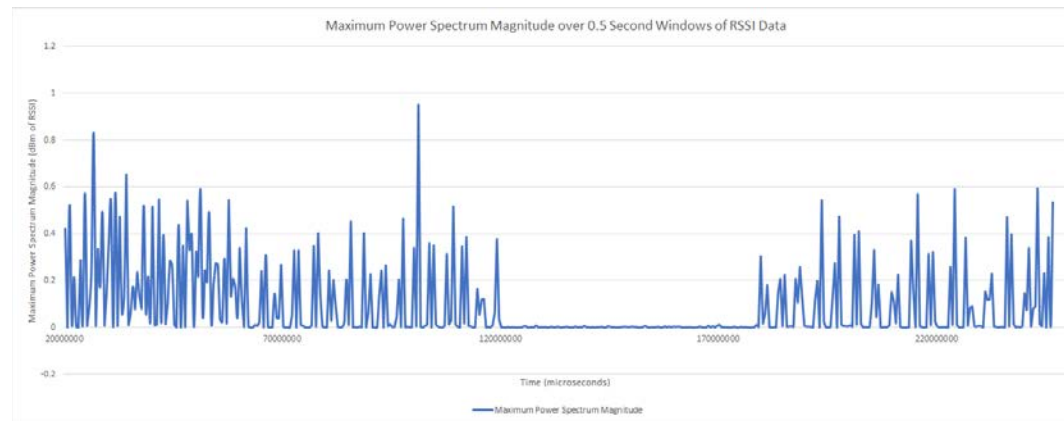
## Feature Extraction from Physical Properties of RFID

- We limit our training observations to the “biologically feasible” class only.
  - For example, no training data are collected from “non-breathing” periods.
  - Some environmental deployment properties are unknown prior to observing data, so semi-supervision (unlabeled observation of normal use) is necessary in order to establish baseline data from which subject state changes are determined.
  - Thus, we do not train the classifier on the subject’s activity states, but rather only on environmental noise.
- Further, we limit any use of perceptron-based classifiers (*i.e.*, Support Vector Machine) to a low-dimensional feature space, because the amount of training data required increases exponentially with the feature dimension.
  - 2.3 minutes of training data are needed for a 1% error tolerance with 95% confidence.
- To evaluate features computed from the RF physical properties, we use the Fisher Linear Discriminant Ratio (FDR).



## Feature Extraction from Physical Properties of RFID

- RF energy absorbed by the body results in a dynamic range of 1-2 dBm as opposed to 5-10 dBm (2-5 feet away) when held away from the body, sacrificing feature separability.
- RSSI mean and standard deviation of short windows (0.5-4.0 seconds) of data provided limited separation, which improved with the length of the window.
  - Longer windows sacrifice real-time processing performance.
- Much of the separability lost in the data is attributable to the mixing of non-actuating periods even during the “breathing” state, due to pauses in-between breaths.
  - The Discrete Fourier Transform (DFT) yields the maximum magnitude at a given frequency for short windows of data.
  - The maximum DFT magnitude has a Fisher score of 0.49 when separating between classes, but a score of 3.85 if the data in-between breaths are removed from the breathing class samples.



## Outline

- Introduction and Background
- Secure and Efficient Monitoring of RFID-Based Devices
- Feature Extraction from Physical Properties of RFID
- **State Classification**
- Rate Estimation
- Prediction
- Experimental Protocol
- Conclusions and Contributions

} Processing and  
Visualization Layer



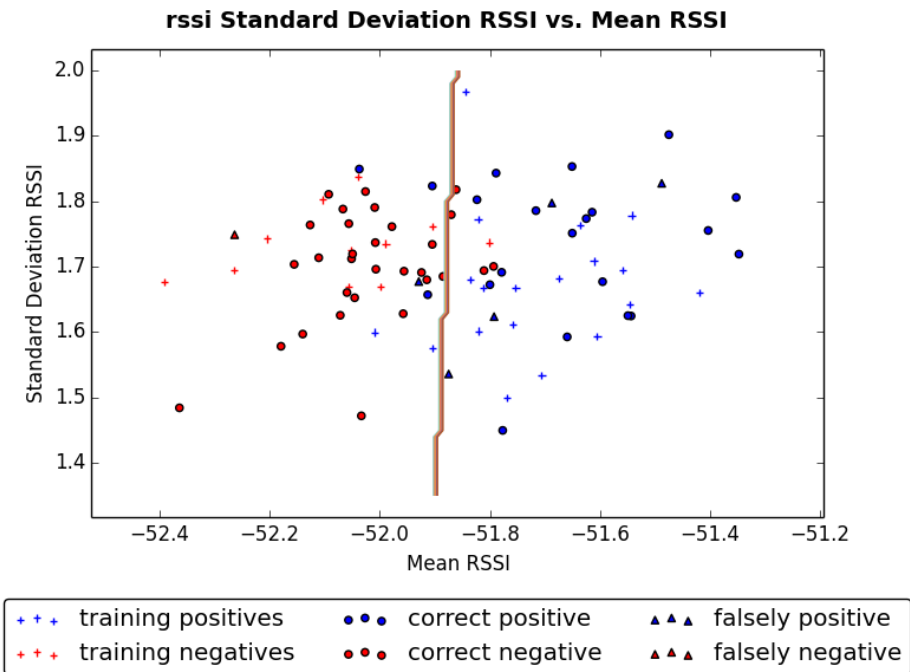
DREXEL UNIVERSITY

College of

Engineering

# Overcoming Feature Imbalance in Biomedical Classification

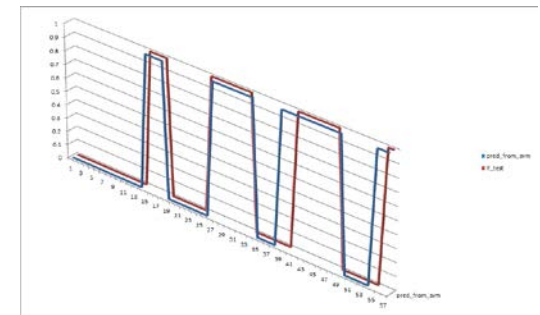
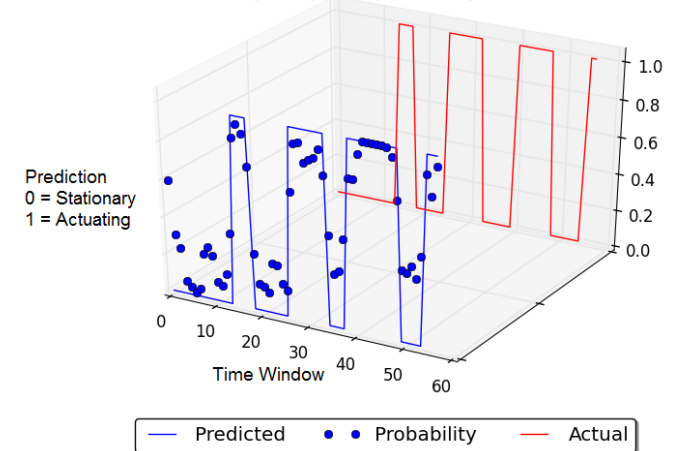
- Synthetic anomaly generation enables Two-Class Support Vector Machine (SVM) for classification, which is advantageous over a One-Class Support Vector Machine when the relationship between the anomaly data and the observed data is known.
  - For example, we know that the anomaly data should appear away from the extreme end of the normal data on one side only.
  - One-Class SVM classifiers are rigid in classifying data outside of the observed margin, and identify anomalies in any direction away from the margin.
- A Two-Class SVM enables likelihood estimation of each prediction based on its distance from the two class centroids.



## State Classification Using RFID Features

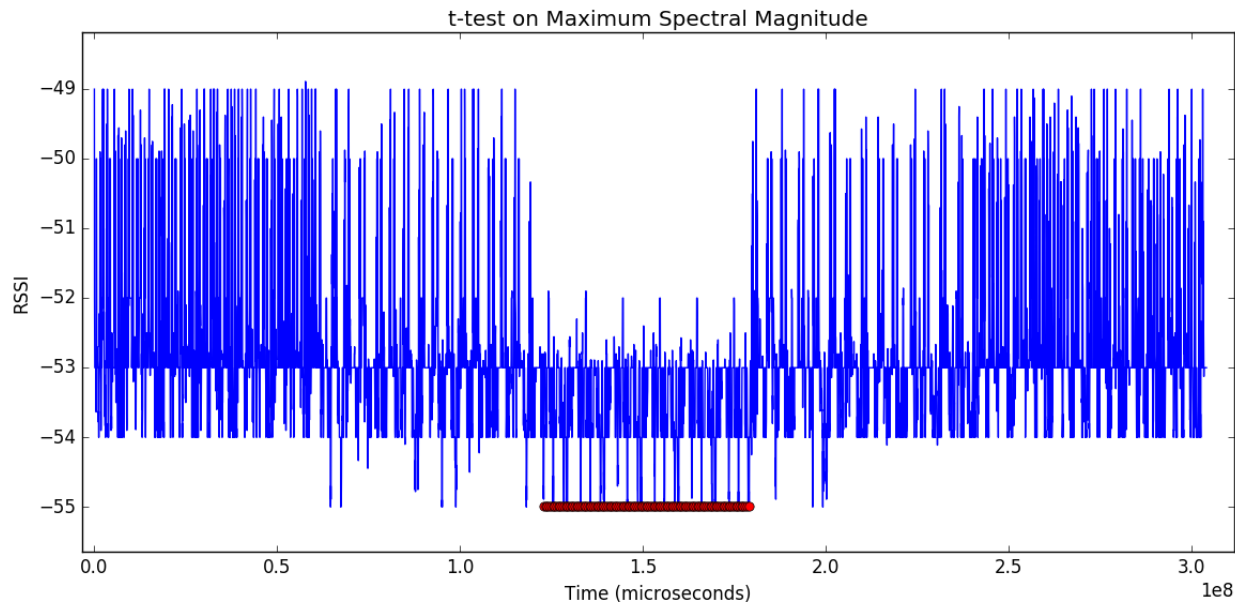
- To classify immediate strain gauge state, a Support Vector Machine (SVM) is used with semi-supervised training data.
- Synthetic anomalies are generated and injected into the data, enabling the use of a Two-Class SVM, overcoming the limitations of a rigid omnidirectional boundary of a One-Class SVM.
- Platt Scaling enables classification at a probabilistic threshold, via logistic regression with weights fit using isotonic regression.
- We observed faster classification of respiratory cessation and an improvement over One-Class SVM classification from a Receiver Operating Characteristic (ROC) Area-under-the-Curve (AUC) from 0.71 to 0.94.

Predicted and Actual Classifications over time with superimposed posterior probabilities



## State Classification Using RFID Features

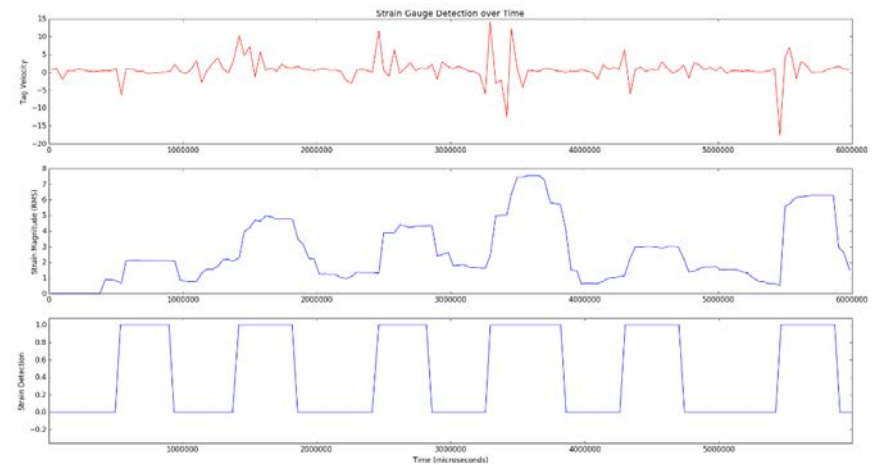
- For non-perceptron semi-supervised detection of long-term state events (*i.e.*, apnea), we use a hypothesis test on the spectral magnitude of the RSSI departure from the local mean, whose t-score is a separable feature.
- Spectral hypothesis testing enables a shorter window than the perceptron, at the cost of spectral leakage that results from the shorter window.



## State Classification Using RFID Features

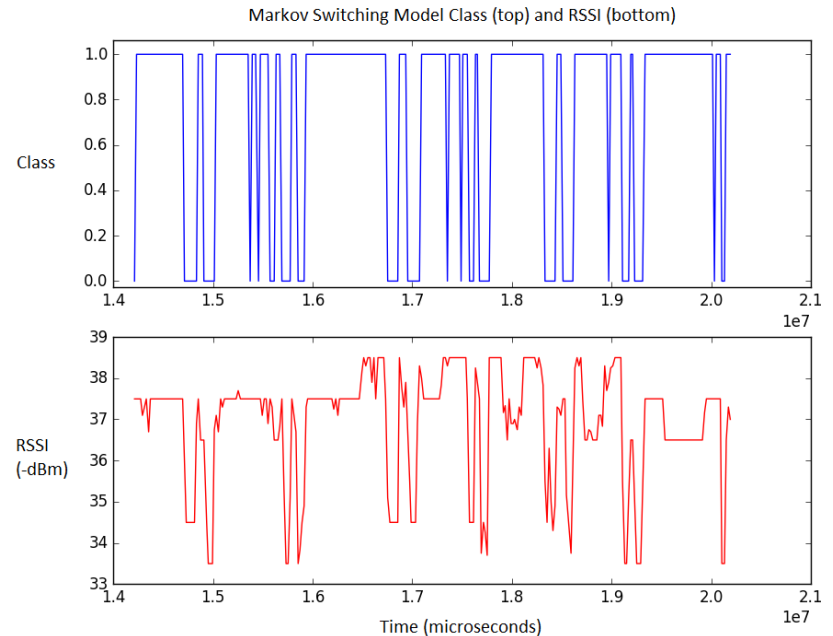
- For discrete events (*i.e.*, uterine monitoring, individual respiration detection), the first order difference of the correlation between the observed RSSI and tag velocity is used to state change and duration detection, which correlate more strongly during strain motion.
- Inflection points on the sliding root-mean-square of  $\delta$  are used to identify band strain.
- Correlation classification improved significantly over individual feature analysis.
  - The velocity measure improved (ANOVA  $p < 0.0001$ ) over  $\zeta$  alone for detection of the start and end of a strain motion
  - $\zeta$  improved over the velocity measure for classifying true respirations (ANOVA  $p = 0.001$ ).
  - Events were identified within 0.57 seconds by Root Mean Squared (RMS) error.

$$\delta = \text{corr}(\Delta\zeta, \Delta v) = \frac{\text{cov}(\Delta\zeta, \Delta v)}{\sigma(\Delta\zeta)\sigma(\Delta v)}$$



# State Classification Using RFID Features

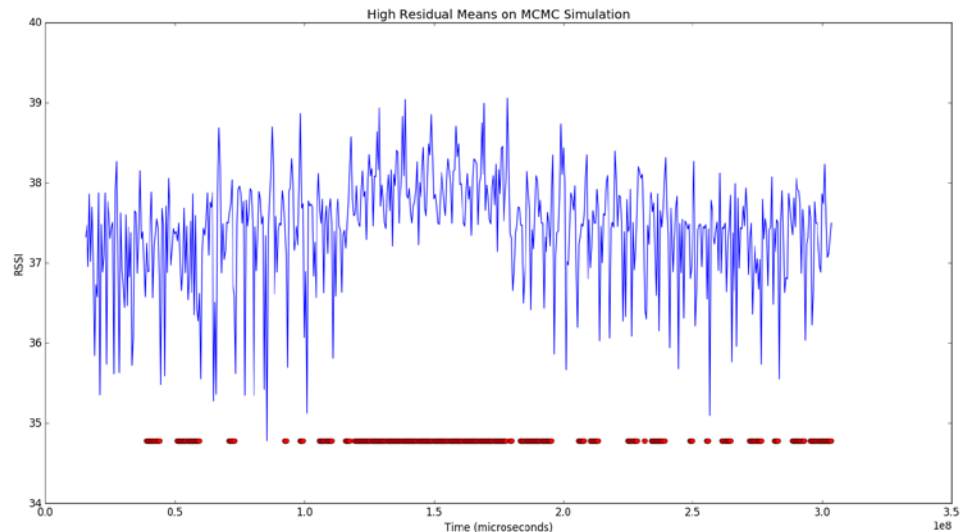
- Using the relationship between power and velocity for activity detection, such as that observed during respiration, uterine activity or movement of the extremities, a Hidden Markov Model (specifically, a Markov Switching Model) is fit with semi-supervised data that can contain samples from each class without knowledge of the classes themselves.
- A tuple  $[d, r, \zeta, v]$  representing the Doppler, RSSI delta from mean, calibrated  $P_{rx}$ , and velocity-by-phase, is used to fit the model.
- The Markov Switching Model applies a Maximum Likelihood Estimate (MLE) of each tuple belonging to one of a set of classes  $\theta$  (i.e., band stretching or stationary).



$$l(\theta|x; \hat{\theta}) = \sum_{\theta \in \hat{\theta}} (-1)^\theta [(x - \mu_\theta)^T \Sigma_\theta^{-1} (x - \mu_\theta)^T + \ln(\Sigma_\theta)]$$
$$\theta = \underset{\theta \in \hat{\theta}}{\operatorname{argmax}} l(\theta|x; \hat{\theta})$$

## Determining Dynamic Retraining Conditions

- Like a Markov Switching Model, we use a Markov Chain Monte Carlo (MCMC) simulation to search for the existence of two distributions of data within the window.
- The Markov Switching Model does this by building a semi-supervised model of data using gradient descent, and may converge to a local optimum.
- MCMC uses unsupervised search, and monitors the changing properties of the identified distributions.
- By observing changes in the properties of the identified distributions, we can detect point-in-time changes to the environment or subject that may require retraining (*i.e.*, mean trend).
- MCMC also classifies each data point within the window to one of the distributions.



## Determining Dynamic Retraining Conditions

- Using MCMC and the hypothesis score on maximum spectral magnitude, we vote on the following retraining conditions (including apnea) to determine a change in environment or subject:
  - Mean or variance of the stretching distribution
  - Mean of the non-stretching distribution
  - Number of distributions detected
  - Percentage of data points most likely to fit in the stretching distribution
  - $P_{rx}$  spectral t-score 95% outlier
  - Prolonged single-state output by the Markov Switching Model
- If any single condition persists for N continuous windows, voting is overridden by that alert.

	<b>First Apnea (t=30 sec) Detection Time</b>	<b>Second Apnea (t=90 sec) Detection Time</b>	<b>False Positive(s)</b>
<b>Rate 10</b>	37 sec	91 sec (brief), 97 sec	65-68 sec
<b>Rate 15</b>	45 sec	103 sec	71 sec
<b>Rate 20</b>	37 sec	98 sec	64 sec
<b>Rate 30</b>	34 sec	98 sec	None
<b>Rate Varied</b>	39 sec	113 sec	29 sec



# Outline

- Introduction and Background
- Secure and Efficient Monitoring of RFID-Based Devices
- Feature Extraction from Physical Properties of RFID
- State Classification
- **Rate Estimation**
- Prediction
- Experimental Protocol
- Conclusions and Contributions

} Processing and  
Visualization Layer



## Rate Estimation

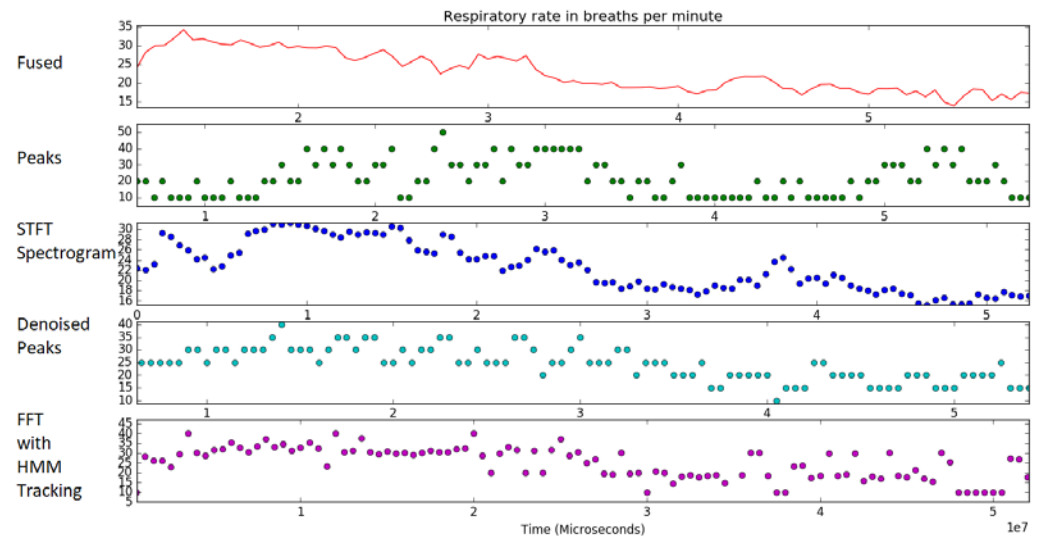
- To estimate respiratory rate, we fuse discrete signal information with spectral measurements.
  - For example, changes in classification and maximum spectral magnitude
- A Short-Time Fourier Transform is used on a sliding window of RSSI data, considering those magnitude peaks corresponding with the most centered frequency by phase.
  - To account for spectral leakage, the spectral centroid, a weighted average of the frequency by spectral magnitude, is taken for the final spectral frequency estimate.
- Taken independently, each rate estimation measurement is subject to perturbations due to environmental noise (*i.e.*, multipath, subject movements) and process noise (*i.e.*, spectral leakage or rounding error due to quantization).
  - However, each estimate is informative of the true underlying measurement, and can be fused via a probabilistic multivariate mixture model.

$$K = \forall_{x \in F} | F[x] \geq \frac{1}{2} F[k]$$
$$k = \operatorname{argmin} K | p[k] = \min p[K]$$
$$f' = \frac{\sum_{i=k-w}^{k+w} f_i F_i}{\sum_{i=k-w}^{k+w} F_i}$$



# Multi Measure Fusion for Robust Rate Estimation

- We perform Expectation Maximization (EM) on a Gaussian Mixture Model (GMM) constructed from point estimates from each measurement approach.
  - Local variances are used to estimate the uncertainty within each estimate.
  - The likelihood of each measurement is computed within the GMM, and the final fused estimate is a weighted average of the individual point estimates by their likelihood.
- If the true rate changes, the variances of all estimates should shift together, barring individual estimation error.
  - A full covariance matrix is provided to the GMM model, modeling the change in variance of each pair of measurements as well as the individual measurement variances.



## Multi Measure Fusion for Robust Rate Estimation

Spectral Centroids RMS Error	Peak Detection RMS Error	GMM RMS Error
11 bpm	9 bpm	6 bpm

- Variance is reduced by  $\sim 2/3$  standard deviations from the mean of the measure variances.
- Fusion was not destructive in any case by Root Mean Squared Error, and was, at times, within rounding error of optimal.
- Average estimate error for human trials using 15 rate varying scenarios is given below:

FFT with HMM Avg RMS Error	Peak Detection Avg RMS Error	Spectral Centroids Avg RMS Error	GMM Avg RMS Error
6.0 bpm	5.0 bpm	3.8 bpm	3.6 bpm



# Outline

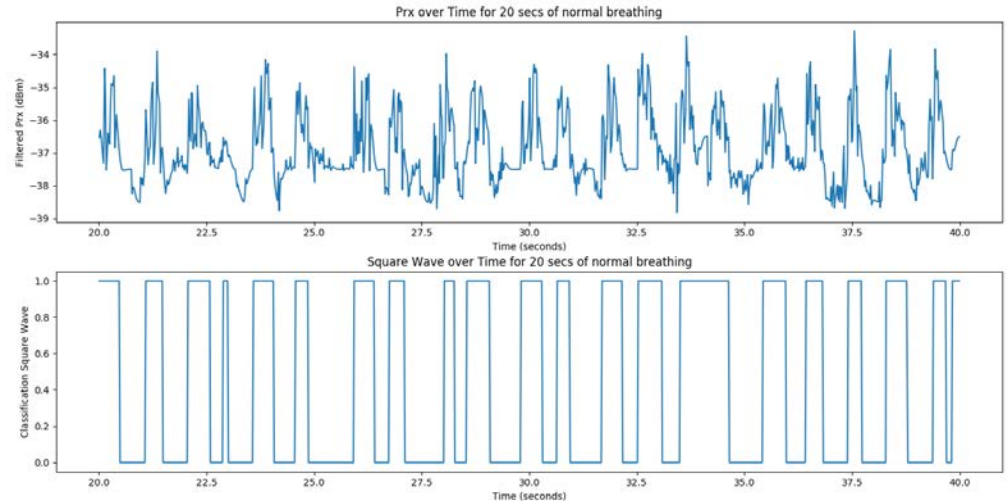
- Introduction and Background
- Secure and Efficient Monitoring of RFID-Based Devices
- Feature Extraction from Physical Properties of RFID
- State Classification
- Rate Estimation
- **Prediction**
- Experimental Protocol
- Conclusions and Contributions

Processing and  
Visualization Layer



## Actionable Prediction of Next Respiratory Activity

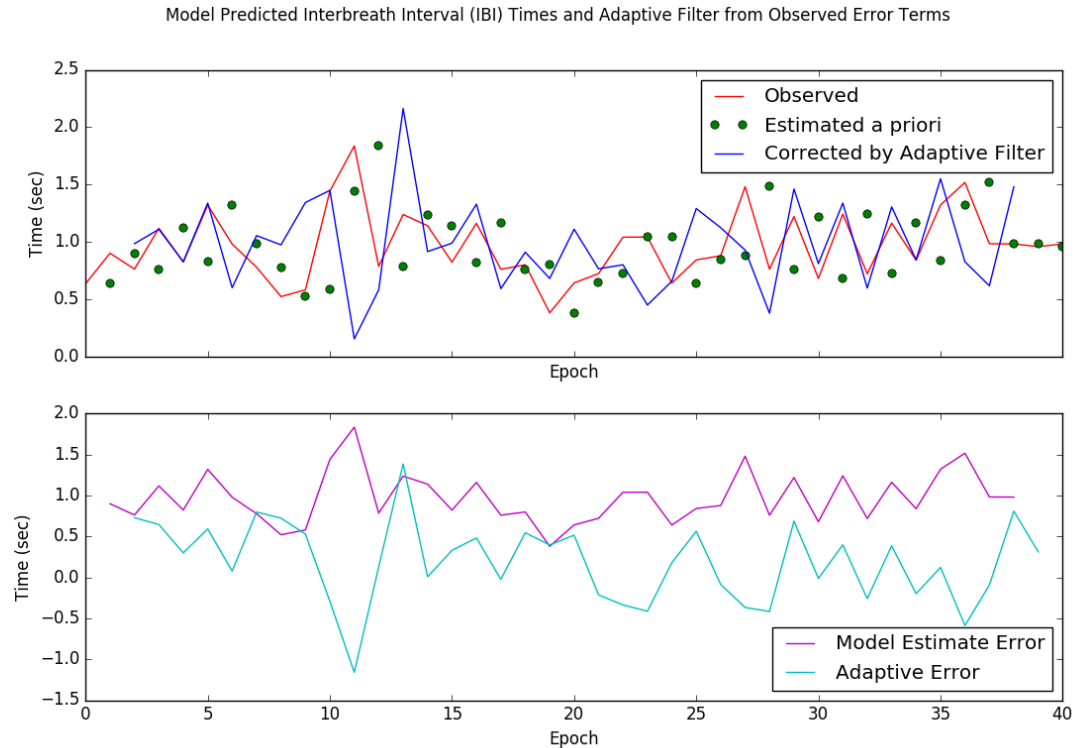
- A log-normal distribution of infant respiratory activity has been observed in the literature, which has been fit using an autoregressive model.
- We applied this model to sample respiratory data to predict the most likely time of the onset of the next breath.
- To determine the beginning of each breath, the Markov Switching Model was applied to generate a square wave, compressing high-frequency fluctuations into a single pulse.



- An affine projection adaptive filter uses Lagrangian constrained optimization to favor small changes to the filter while correcting the most recent observation error to 0.

# Actionable Prediction of Next Respiratory Activity

- IBI instability is a predictor of an apnea event in preterm infants (Salisbury, *et al. J Appl Physiol* 1985; 107(4): 1017-1027).
- Ventilator equipment is intrusive.
- Instantaneous changes in rate can be detected using rate detection algorithms.
- Adaptive filter slightly worse overall in RMS error, but improved after converging.
  - RMS error of 0.4 seconds.



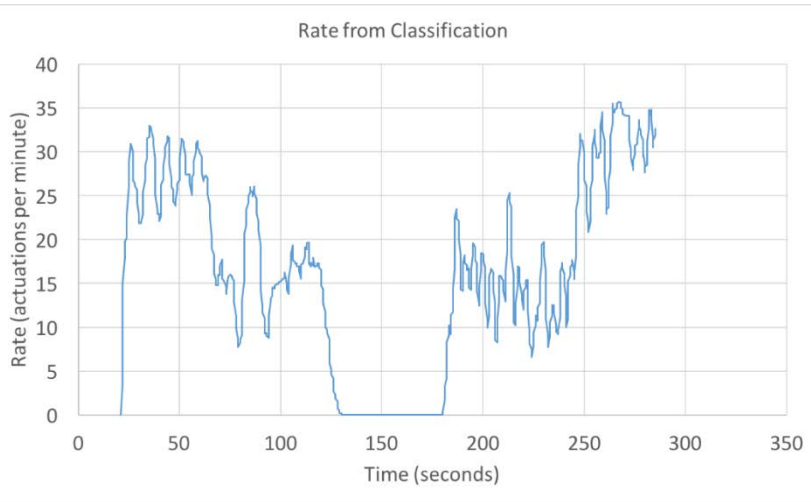
## Outline

- Introduction and Background
- Secure and Efficient Monitoring of RFID-Based Devices
- Feature Extraction from Physical Properties of RFID
- State Classification
- Rate Estimation
- Prediction
- **Experimental Protocol**
- Conclusions and Contributions



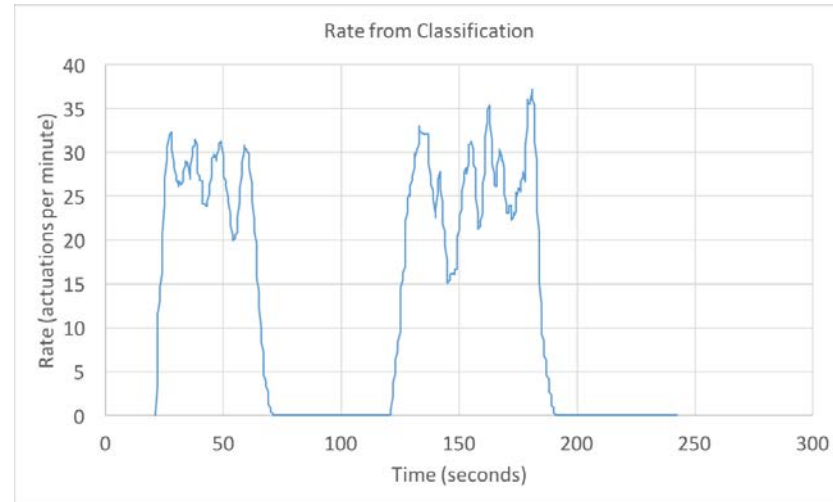
# Experimental Protocol and Human Subjects Testing

- A Laerdal SimBaby was used for simulated laboratory testing. The SimBaby can be programmed using various scenarios to implement biologically undesirable phenomena that we can detect using the wearable smart garment Bellyband device.
- The SimBaby was programmed to breathe at a predefined rate for a predefined period (*i.e.*, 30 breaths per minute for 30 seconds, followed by 15 breaths per minute for 30 seconds), interjecting prolonged periods of apnea in-between.



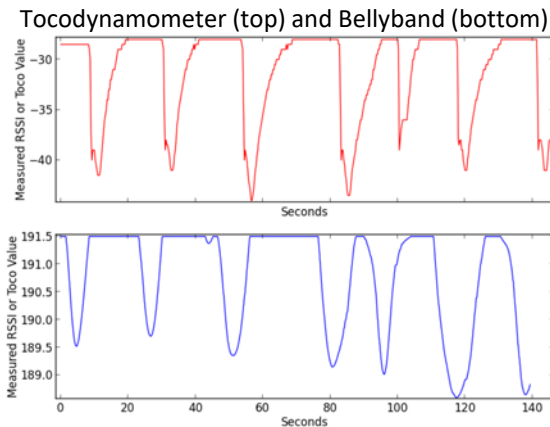
Rate 30-0-30-0,  
1 min each  
(right)

20  
seconds  
baseline  
data



# Experimental Protocol and Human Subjects Testing

- Additionally, a Philips 50XM Tocodynamometer was used for uterine activity comparison, and a respiratory pressure monitor was used to capture ground truth from the SimBaby.
- The 50XM was integrated into the IoT sensor network software framework to facilitate data collection from each device.
- Visual contraction information was collected from the tocodynamometer pressure sensor and RFID Bellyband for visual comparison, as would be seen in a hospital setting during labor and delivery.



## Experimental Protocol and Human Subjects Testing

- Additionally, an infant human respiratory protocol (IRB 1504003601) and adult human heart/respiratory protocol (IRB 1604004440) have been implemented to collect human subjects data.
- A third protocol is approved for uterine monitoring during labor and delivery (IRB 1504003602).
- Adults are asked to breathe normally, with respiratory activity tracked by counting breaths or using a respiratory monitor for ground-truth monitoring.
- Infant respiration is noted on the monitoring equipment at the NICU for comparison.
- Interrogation distance is currently 50 to 100 cm from the body.
  - At these distances, the maximum peak Specific Absorption Rate (SAR) is at most 0.25 W/kg.
  - The maximum allowable SAR is 0.8 W/kg.
- The power exposure at these distances is at most 0.03 mW/cm<sup>2</sup>.
  - The Federal Communications Commission (FCC) publishes a Maximum Permissible Exposure (MPE) of 0.6 mW/cm<sup>2</sup> in the 900 MHz band.



## Outline

- Introduction and Background
- Secure and Efficient Monitoring of RFID-Based Devices
- Feature Extraction from Physical Properties of RFID
- State Classification
- Rate Estimation
- Prediction
- Experimental Protocol
- **Conclusions and Contributions**



## Conclusions and Contributions

- We provide a software framework for the real-time collection of physical properties of heterogeneous IoT sensor networks.
  - This includes contributable modifications to physical layer libraries for RFID data collection.
- These software frameworks have also been used to support other RFID-based IoT sensor systems, including RFID-based heart monitoring and limb movement monitoring to detect the onset of symptoms of deep venous thrombosis (DVT).
- We also provide a pluggable software framework for statistical processing and multi-estimate fusion on physical properties of single-tag, single-interrogator RF physical properties to infer wearer state, integrating securely with the physical layer framework.

Real-Time Sensor Fusion of Algorithmic Sensors

Predictive  
Classification

Real-Time State  
Estimation

Adverse Condition  
Alerting

Secure Software Framework for Unobtrusive Monitoring of IoT  
Devices



## Conclusions and Contributions

- We developed, tested, and compared adaptive and predictive algorithms for a wearable strain-gauge sensor applicable to a variety of use cases.
- We mitigated the effects of quantization, environmental noise, and mechanical noise, by performing multi-measurement fusion on these individual algorithms, combining them in real-time to establish a more accurate estimate of wearer state.
  - By generating synthetic anomaly data, we enable semi-supervised training of traditional classifiers, allowing for multi-classifier fusion algorithms that operate on multiple tags (*i.e.*, sensor networks or reference antennas).
  - Our approach yielded statistically significant improvements in classification and state monitoring of passive wireless wearable smart garment devices.

Real-Time Sensor Fusion of Algorithmic Sensors

Predictive  
Classification

Real-Time State  
Estimation

Adverse Condition  
Alerting

Secure Software Framework for Unobtrusive Monitoring of IoT  
Devices



DREXEL UNIVERSITY

College of

Engineering

## Accepted Publications

- Sayandeep Acharya, **William M. Mongan**, Ilhaan Rasheed, Yuqiao Liu, Endla Anday, Genevieve Dion, Adam Fontecchio, Timothy Kurzweg, and Kapil R. Dandekar. **Ensemble Learning Approach via Kalman Filtering for a Passive Wearable Respiratory Monitor**. IEEE Transactions of Biomedical and Health Informatics, to appear July 2018.
- **William M. Mongan**, Robert Ross, Ilhaan Rasheed, Yuqiao Liu, Khyati Ved, Endla Anday, Kapil Dandekar, Genevieve Dion, Timothy Kurzweg, and Adam Fontecchio. **Data Fusion of Single-Tag RFID Measurements for Respiratory Rate Monitoring**. IEEE Signal Processing in Medicine and Biology (SPMB) 2017, December, 2017.
- Shrenik A. Vora, **William M. Mongan**, Endla K. Anday, Kapil R. Dandekar, Genevieve Dion, Adam K. Fontecchio, and Timothy P. Kurzweg. **On Implementing an Unconventional Infant Vital Signs Monitor with Passive RFID Tags**. IEEE International Conference on RFID, 2017, May, 2017.
- **William Mongan**, Ilhaan Rasheed, Khyati Ved, Shrenik Vora, Kapil Dandekar, Genevieve Dion, Timothy Kurzweg, and Adam Fontecchio. **On the Use of Radio Frequency Identification for Continuous Biomedical Monitoring**. ACM/IEEE International Conference on Internet-of-Things Design and Implementation (IoTDI) 2017, April, 2017.
- **William M. Mongan**, Ilhaan Rasheed, Khyati Ved, Ariana Levitt, Endla Anday, Kapil Dandekar, Genevieve Dion, Timothy Kurzweg, and Adam Fontecchio. **Real-Time Detection of Apnea via Signal Processing of Time-Series Properties of RFID-Based Smart Garments**. IEEE Signal Processing in Medicine and Biology (SPMB) 2016, December, 2016.
- **William Mongan**, Endla Anday, Genevieve Dion, Adam Fontecchio, Tim Kurzweg, Yuqiao Liu, Owen Montgomery, Ilhaan Rasheed, Cem Sahin, Shrenik Vora, and Kapil Dandekar. **A Multi-Disciplinary Framework for Continuous Biomedical Monitoring Using Low-Power Passive RFID-based Wireless Wearable Sensors**. Proceedings of the IEEE Smart Systems Workshop 2016, May, 2016.
- Shrenik Vora, **William Mongan**, Kapil Dandekar, Adam Fontecchio, and Tim Kurzweg. **Wireless Heart and Respiration Monitoring for Infants through Passive RFID Tags**. International Conference on Biomedical and Health Informatics (BHI), February, 2016.
- Damiano Patron, **William Mongan**, Timothy Kurzweg, Adam Fontecchio, Genevieve Dion, Endla Anday, and Kapil R. Dandekar. **On the Use of Knitted Antennas and Inductively Coupled RFID Tags for Wearable Applications**. IEEE Transactions on Biomedical Circuits and Systems, January 2016.



# Accepted Posters, Invited Talks, Grants and Funding Support

- Accepted Posters
  - **William Mongan**, Kapil R. Dandekar, Genevieve Dion, Timothy Kurzweg, and Adam Fontecchio. **Statistical Analytics of Wearable Passive RFID-based Biomedical Textile Monitors for Real-Time State Classification**. *IEEE Signal Processing in Medicine and Biology (SPMB) Symposium Poster*. Philadelphia, PA. December, 2015.
- Invited Talks
  - Owen Montgomery, **William Mongan**, Ilhaan Rasheed, Khyati Ved, Shrenik Vora, Kapil Dandekar, Genevieve Dion, Adam Fontecchio, and Timothy Kurzweg. **Wearable Technology Advances Health for Mothers and Babies**. *Yale Tech Summit*. New Haven, CT. October, 2016.
- Grants and Funding Support
  - Adam K. Fontecchio and **William M. Mongan**, co-Principal Investigators. Analytics on Real-Time Biometrics from Passive Wearable Smart-Garments; 2017-2018, Commonwealth Universal Research Enhancement (CURE) Formula Grant (SAP117558-014), \$75,000.
  - **William M. Mongan** and Adam K. Fontecchio. Drexel University Co-op Funding Award supplement to support undergraduate experiential learning in research; 2017-2018, \$7,250.



## Publications in Preparation

- **William M. Mongan**, Ilhaan Rasheed, Robert Ross, Kapil R. Dandekar, Genevieve Dion, Timothy Kurzweg, and Adam K. Fontecchio. **Real-Time Detection of Motion-Based Events Using RFID Tags in Wireless Wearable Garment Devices.**
- Robert Ross, **William M. Mongan**, Patrick O'Neill, Ilhaan Rasheed, Adam Fontecchio, and Kapil R. Dandekar. **An Adaptively Parameterized Algorithm Estimating Respiratory Rate from a Passive RFID Smart Garment.**
- Patrick O'Neill, **William M. Mongan**, Robert Ross, Ilhaan Rasheed, Kapil R. Dandekar, and Adam K. Fontecchio. **An Adaptive Search Algorithm for Detecting Respiratory Artifacts Using a Wireless Passive Wearable Device.**
- Austin Gentry, Brent Lee, **William M. Mongan**, Owen Montgomery, and Kapil Dandekar. **Activity Segmentation Using Wearable Sensors for Deep Vein Thrombosis Condition Detection.**
- Khyati Ved, Ilhaan Rasheed, **William Mongan**, Genevieve Dion, Timothy Kurzweg, Adam Fontecchio, and Kapil R. Dandekar. **Ambient Motion Detection Using RFID-Based Smart Garments.**



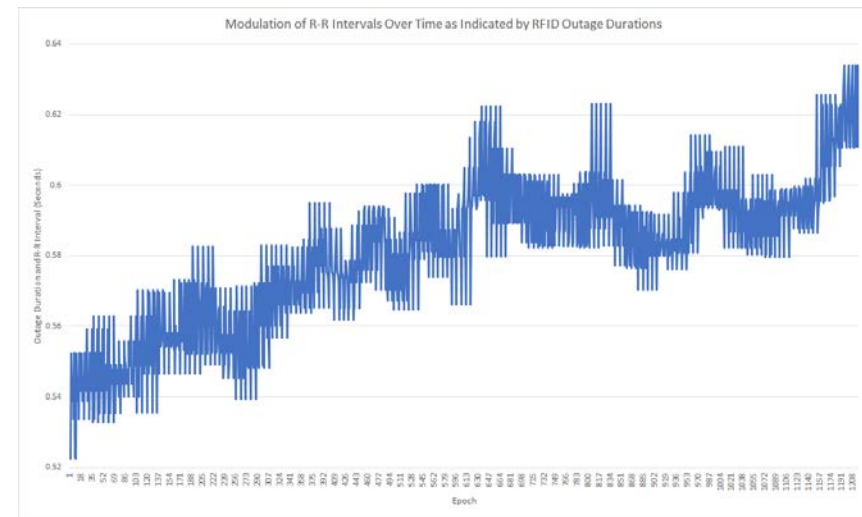
DREXEL UNIVERSITY

College of

Engineering

## Future Work

- We are integrating multiple knit antennas for multi-sensor fusion by observing, modeling, and then mitigating the environmental noise from the main respiratory tag.
- We will study the effects of band placement, body composition, and band fit on the physical properties returned from an RFID Bellyband, to deterministically reduce noise artifacts due to these causes.
- We will evaluate RF communications beyond RFID for biomedical state monitoring.
- We are evaluating the use of RFID-based passive heart monitors as a respiratory monitoring estimate.



## Thanks!

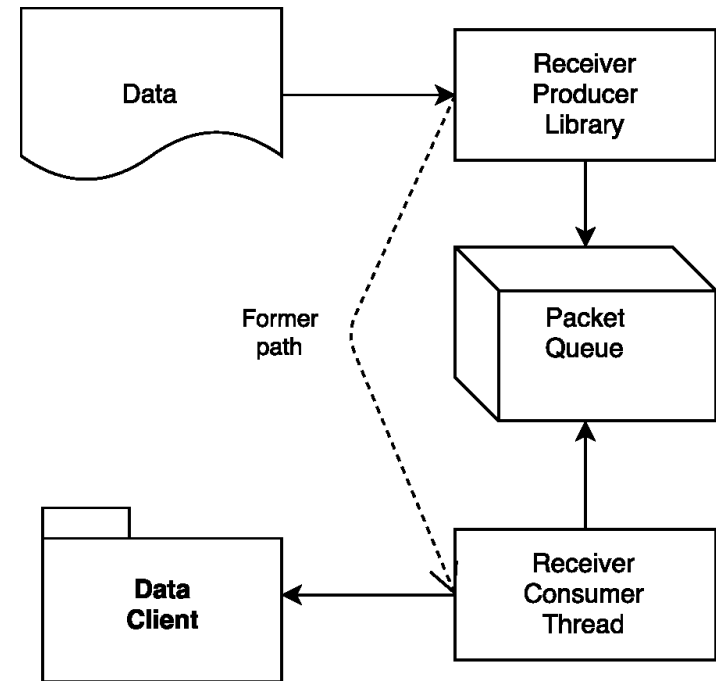
- My advisor: Adam Fontecchio
- My committee: Kapil Dandekar, Genevieve Dion, Naga Kandasamy, and Tim Kurzweg
- Guiding domain collaborators: Endla Anday, Vineet Bhandari, Kelly Joyce, Owen Montgomery, Michael Weingarten
- Our very multidisciplinary lab: Sayandeep Acharya, Chelsea Knittel, Ariana Levitt, Yuqiao Liu, Ilhaan Rasheed, Khyati Ved, Shrenik Vora
- Students I have co-advised through this project: Semanti Basu, Samantha Bewley, Rachel Goken, Stephen Hansen, Brent Lee, Christopher Lynch, Robert Ross, Patrick O'Neill, Har Patel
- High School teachers we have collaborated with: Michael Darfler, Kyle Ellis, Barbara Matas, Anna Schall
- Funding sponsors: The National Science Foundation, The National Institutes of Health, The Commonwealth of Pennsylvania, Drexel University Steinbright Career Development Center
- ... and you!



# Appendix

## Physical and Sensing Layer

- The Producer-Consumer pattern uses a message queue that is populated by the interrogator ("the producer"), and emptied in First-In-First-Out (FIFO) order by the client ("the consumer"), each at independent rates.
- The message queue is constructed to be elastic and blocking, so that the client is held until data is available if it exhausts the message queue, and the queue expands dynamically to support the interrogator if its interrogation rate is higher than the client read rate.
- Top-Half/Bottom-Half processing and overriding default network transport behavior (Nagle's algorithm) enables real-time processing.



## Feature Extraction from Physical Properties of RFID

- FDR computes the ratio of the squared difference of the means to the sum of the variances of data in each “class.”
  - A feature is more cleanly separable between classes if the mean of each class is far apart, and the variances are small enough to avoid overlap at the tails.
  - Since it is biologically infeasible to collect “breathing” and “non-breathing” class samples, we use a Laerdal SimBaby mannequin to simulate these states.
- We observed that separability varied with the respiratory rate, with higher respiratory rates yielding better separability between classes.
  - There are fewer, and shorter, periods in between breaths at higher respiratory rates, such that there are fewer “non-breathing” data points mixed in with the “breathing” class.



## State Classification Using RFID Features

- Low Fisher scores indicate greater potential for overlap among the data between classes during classification.
- Raw spectral analysis may be inaccurate due to the noise embedded in the spectrum of interest, and imprecise due to the frequency spacing resulting from the short windows used for real-time processing.
- Temporal relationship information will be exploited for state classification, by establishing a semi-supervised baseline.
  - 20 seconds of data are observed under “normal” conditions (*i.e.*, normal respiratory activity).
- If 95% outliers below the mean are observed for a period of 10 seconds (the definition of apnea) or more, an apnea condition is observed.

# State Classification Using RFID Features

- Why these classifiers?
  - Each classifier was effective but has potential limitations.
    - Aggregate perceptron classifiers require more training data, balanced training data (which we overcome with synthetic generation), and work better as the training size and window size increase.
    - Spectral classification requires a short enough window for real-time performance, but a long-enough window for spectral resolution, which we overcome for now by considering the overall spectral density as it changes over time via a t-test.
    - Discrete correlation uses temporal information from changes in the signal phase over time to denoise the input signal before classification, which a Hidden Markov Model extends by comparing these changes against a training model, but requires training data and may converge to a local optimum.
    - MCMC requires no training and performs local classification data point by data point, and is conducive for monitoring trends for retraining, but individual data points perturbed by noise will not be filtered out by MCMC as it is with aggregate approaches such as the others.
  - We did not fuse the perceptron because of the window size, but the synthetic anomaly generation will enable fully supervised classification such as multi-knit antenna fusion approaches.



# Overcoming Feature Imbalance in Biomedical Classification

- Existing methods, such as the SMOTE method, exist to overcome challenges in performing classification when an imbalance exists in the training data.
  - This is often the case when detecting anomalies.
  - These methods assume that at least some example reference data exists for all observable classes.
- We adapt this approach and generate synthetic anomaly data for the infeasible class using properties of the observed training data.
- Selected “breathing” class data are reflected about an axis defined by the smallest observed mean, and the mean of the observed standard deviations.
  - Only those data greater than the mean of all windows are reflected, so as to avoid fitting data observed during transitional periods in-between each breath.
- To overcome the imbalance between the classes, and to allow for overlap between the classes, additional training points are generated by sampling from a normal distribution centered at the 5<sup>th</sup> percentile of the means, and the standard deviation of the means.



## Determining Dynamic Retraining Conditions

- Because we do not utilize fully supervised training data samples to identify anomalies in wearer state, but rather compare changes in the feature space over time, it is necessary to monitor the underlying environmental baseline for changes that require a re-configuration of the environmental parameters.
- For example, if new objects appear in the room, or if the wearer makes major movements toward or away from the interrogator, these would need to be recalibrated for future classification and detection.
- Unfortunately, these changes in baseline appear in-band with changes in physical RFID backscatter properties due to strain motion on the Bellyband device.
- As a result, we use a Markov Chain Monte Carlo (MCMC) simulation to detect one or two distinct distributions of data within each window.

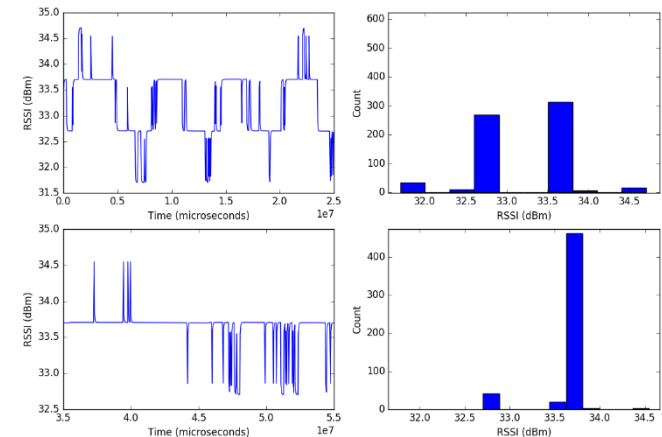


## Determining Dynamic Retraining Conditions

- The MCMC simulation optimizes the goodness of fit within the identified distributions, and converges on a solution after a certain number of iterations  $N$ .
  - Convergence will be optimal as  $N \rightarrow \infty$ .
- There are  $2 * 10^{32}$  combinations of 30 data points (0.5-1.0 second of data), which is infeasible for exhaustive search.
- Rather than rely on semi-optimal convergence, we utilize properties of the data points most likely to fit to each identified distribution, and observe their changes over time as a higher order feature.
- Specifically, the mean of each distribution is monitored over time for significant shifts from that observed during baseline configuration.

## Rate Estimation

- Additionally, discrete methods such as significant ( $> 3 \sigma$ ) peak detection over  $\zeta$  and  $corr(\Delta\zeta, \Delta v)$  are used to estimate respiratory rate.
- For comparison with spectral centroids, Hidden Markov Model is applied to the frequency estimate to eliminate large fluctuations in the frequency due to noise, accounting for temporal progression in respiratory rate throughout the sliding window to compute a maximum a posteriori likelihood spectral frequency estimate.
- A biased frequency estimation by Quinn is also applied that reduces estimation error variance due to spectral leakage to near the Cramér-Rao bound.
- Generally, spectral centroids outperformed both of these estimates, but not in all cases; maximum likelihood fusion from these estimates will be used to form an improved rate estimate.



## Multi Measure Fusion for Robust Rate Estimation

- The GMM fuser weights each measurement according to its Fisher information, but uses maximum likelihood estimation by using each measurement's local history variance as a measure of uncertainty.
  - This allows EM "fusion" even for a single measurement.
  - EM estimates are smoothed with a Kalman filter that weights process variance over measurement noise, since measurement noise should be mitigated by the fuser.
- EM is an unbiased estimator, which we form by weighting the minimum variances from the measurements.
  - Choosing the measure with minimum variance would theoretically yield a minimum variance unbiased estimator, we perform weighting to allow for unknown process and measurement noise embedded within these measurements.
- Quinn interpolation bias is reduced to near-minimum RMS error by EM fusion of unbiased estimators such as mean spectral centroids or discrete measures.

# Experimental Protocol and Human Subjects Testing

